

Critical earthquake loads for SDOF inelastic structures considering evolution of seismic waves

Abbas Moustafa¹, Kohei Ueno² and Izuru Takewaki^{2*}

¹*Department of Civil Engineering, Minia University, Minia 61111, Egypt*

²*Department of Urban & Environmental Engineering, Kyoto University, Kyotodaigaku-katsura, Kyoto 615-8540, Japan*

(Received November 24, 2009, Accepted March 24, 2010)

Abstract. The ground acceleration measured at a point on the earth's surface is composed of several waves that have different phase velocities, arrival times, amplitudes, and frequency contents. For instance, body waves contain primary and secondary waves that have high frequency content and reach the site first. Surface waves are composed of Rayleigh and Love waves that have lower phase velocity, lower frequency content and reach the site next. Some of these waves could be of more damage to the structure depending on their frequency content and associated amplitude. This paper models critical earthquake loads for single-degree-of-freedom (SDOF) inelastic structures considering evolution of the seismic waves in time and frequency. The ground acceleration is represented as combination of seismic waves with different characteristics. Each seismic wave represents the energy of the ground motion in certain frequency band and time interval. The amplitudes and phase angles of these waves are optimized to produce the highest damage in the structure subject to explicit constraints on the energy and the peak ground acceleration and implicit constraints on the frequency content and the arrival time of the seismic waves. The material nonlinearity is modeled using bilinear inelastic law. The study explores also the influence of the properties of the seismic waves on the energy demand and damage state of the structure. Numerical illustrations on modeling critical earthquake excitations for one-storey inelastic frame structures are provided.

Keywords: critical excitation; earthquake acceleration; seismic waves; inelastic structures; ductility; damage indices.

1. Introduction

The damage of the structures due to the earthquake ground motion depends primarily on three parameters: (1) the characteristics of the ground motion (magnitude, duration, frequency content, amplitude and local soil type), (2) the properties of the structure (natural frequencies, mode shapes, material of construction, structural system and ductility capacity), and (3) how close the structure's fundamental natural frequency to the dominant frequency of the ground motion. In general, the ground motion characteristics involve large uncertainties and cannot be controlled while the structure's properties have smaller variability and can be managed to some extent. For instance, the material of construction can be selected and the lateral seismic-resistance of the structure can be improved through ductility detailing.

* Corresponding author, Professor, E-mail: takewaki@archi.kyoto-u.ac.jp

The seismic waves arriving at a site depend on the source mechanism, the travel path (site-source distance) and the local soil condition (Der Kiureghian 1996). The ground motion hitting the structure's foundations is composed of several waves that have different phase velocities, arrival times, amplitudes, and frequency contents (e.g. Hudson 1969). Body waves contain P (primary) and S (shear or secondary) waves that have higher frequencies and reach the site first. Surface waves, on the other hand, are composed of Rayleigh (R) and Love (L) waves which have lower phase velocities, lower frequencies and reach the site next. P-waves are compression waves while S-waves are transverse waves. Surface waves result in rolling motion that constitutes the most destructive waves. Some of these waves could be of more damage to the structure depending on their dominant frequency, amplitude and relation with the structure's natural frequencies. The attenuation of the seismic waves that propagate at the source gives rise to variation of the ground motion in time and space. Seismic waves attenuate due to natural causes (local soil amplification, reflection, refraction and energy dissipation of travelling waves) and man-made obstacles, such as, cavities and underground structures (Wang *et al.* 2010). Surface waves are known to attenuate slower than body waves. Attenuation of seismic waves depends largely on soil conditions. For instance, soft soils can significantly amplify the amplitude and modify the frequency content of the ground motion. Attenuation modeling of the ground motion is an active field of research in engineering seismology (see e.g. Elnashai and Sarno 2008). The influence of the high-frequency components of the ground motion on the damage of masonry structures has been studied by Meyer *et al.* (2007). High frequencies can cause vertical interstone vibrations resulting in irreversible relative displacements of the stones, which may ultimately lead to collapse. The partial fluidification and densification of the loose, granular inner core of some unreinforced masonry walls may also increase the outward thrust.

The modeling of strong ground motion has been an interesting problem in earthquake engineering for many decades. A state of the art review on modeling stationary/non-stationary deterministic and stochastic ground motion can be found in He and Agrawal (2008), Takewaki (2007), Conte and Peng (1997), Der Kiureghian and Crempien (1989), Lin and Yong (1987). This aspect is of importance in seismic analysis and design of engineering structures. The Kanai-Tajimi model represents one of the most widely used ground motion models (Lin and Yong 1987). The parameters of the ground motion model are usually estimated by matching the model parameters with recorded accelerograms. Der Kiureghian and Crempien (1989) decomposed the 1971 Orion earthquake into seven acceleration components of different frequency bands. Conte (1992) employed the ARMA stochastic models to study the effect of the frequency nonstationarity of the ground motion on the response of inelastic structures. Conte and Peng (1997) developed a fully non-stationary stochastic model for earthquake accelerations that is composed of several seismic waves.

Strong ground motion involves several uncertainties including time, location, duration, magnitude, frequency content, etc. On the other hand, the structural engineer is often concerned with the worst case scenario that can happen to the structure. The modeling of critical earthquake loads for structures has attracted many researchers. Early research thoughts on this subject have been provided by Drenick (1970), Shinozuka (1970) and Iyengar (1970). Extensive reviews on modeling critical earthquake loads on elastic and inelastic structures have been reported by Takewaki (2001, 2002, 2006, 2007), Abbas and Manohar (2002, 2007), Abbas (2006) and Moustafa (2009a). The notion of critical excitation has been employed recently in identifying critical recorded accelerograms (Takewaki 2005, Amiri and Dana 2005, Zhai and Xie 2007, Moustafa 2009b, Moustafa and Takewaki 2009). Mathematically, the critical input for a given structure is computed

by solving an inverse dynamic problem such that a measure of the structural damage is maximized while the input is constrained to predefined bounds that aim to replicate observed characteristics of recorded ground motions on the input.

This paper models critical ground motion inputs for inelastic structures considering evolution of seismic waves in time and frequency. The ground acceleration is represented as a combination of seismic waves that have different characteristics. The amplitudes and phase angles of these waves are optimized to produce the highest damage in the structure subject to constraints on the peak ground acceleration and energy. The constraints include restrictions on the non-stationary shape and the frequency content of each wave, and bounds on the energy and the peak ground acceleration (PGA) of the total acceleration. The material nonlinearity is modeled using bilinear inelastic relation. The next section demonstrates the dynamic analysis of SDOF inelastic structures to earthquake loads.

2. Dynamic analysis and energies dissipated by inelastic structures

The relative displacement $u(t)$ of a one-storey structure modeled as a SDOF inelastic system driven by the ground acceleration $\ddot{u}_g(t)$ is derived from the equation of motion

$$m\ddot{u}(t) + c\dot{u}(t) + f_s(t) = -m\ddot{u}_g(t) \quad (1)$$

where m and c are the mass and the damping coefficient of the SDOF system and $f_s(t)$ is the inelastic restoring force in the spring which is a nonlinear function of $u(t)$. In other words, the force-deformation relation is no longer a single valued relation. Thus, for a displacement $u(t_i)$, the restoring force depends upon prior history of motion of the system and whether the velocity response $\dot{u}(t_i)$ is increasing or decreasing. The above equation can be reduced to

$$\ddot{u}(t) + 2\zeta\omega\dot{u}(t) + \omega^2 u_y \tilde{f}_s(t) = -\ddot{u}_g(t) \quad (2)$$

where, ζ is the damping ratio, ω is the initial natural frequency for the inelastic system and u_y is the yield displacement. The function $\tilde{f}_s(t)$ is the spring restoring force in a dimensionless form. Referring to Eq. (2), the inelastic response for a given acceleration $\ddot{u}_g(t)$ depends on the initial natural frequency ω , the damping ratio ζ and the yield displacement u_y ($u_y = f_y/k$, $f_y =$ yield strength and $k =$ initial stiffness). The maximum ductility demand is obtained by normalizing the maximum absolute displacement by the yield displacement. The inelastic dynamic response is obtained by solving the incremental equation of motion numerically (Chopra 2007).

The earthquake input energy and the energies stored or dissipated by the structure are quantified by integrating Eq. (1). Thus, the energy balance for the structure is given as (Abbas 2006, Takewaki 2004a, Uang and Bertero 1990, Akiyama 1985, Zahrah and Hall 1984)

$$\int_0^u m\ddot{u}(t)du + \int_0^u c\dot{u}(t)du + \int_0^u f_s(t)du = -\int_0^u m\ddot{u}_g(t)du \quad (3)$$

The right hand side of Eq. (3) represents the input energy to the structure. The first energy term in the left side is the kinetic energy $E_k(t)$

$$E_K(t) = \int_0^u m\ddot{u}(t)du = \int_0^t m\ddot{u}(\tau)\dot{u}(\tau)d\tau = m[\dot{u}(t)]^2/2 \quad (4)$$

The second term in the left side of Eq. (3) is the energy dissipated by damping $E_D(t)$

$$E_D(t) = \int_0^u c\dot{u}(t)du = \int_0^t c[\dot{u}(\tau)]^2d\tau \quad (5)$$

The third term in the left side of Eq. (3) is the sum of the elastic recoverable strain energy $E_S(t)$ and the unrecoverable accumulated hysteretic energy $E_H(t)$ dissipated by yielding

$$E_S(t) = [f_s(t)]^2/(2k); = E_H(t) = \int_0^u f_s(t)du - E_S(t) = \int_0^t \dot{u}(\tau)f_s(\tau)d\tau - E_S(t) \quad (6)$$

The next section demonstrates the use of maximum ductility and hysteretic energy demands in developing damage indices.

3. Quantification of structural damage using damage indices

The literature on damage measures of structures under ground motions is vast (Ghobara *et al.* 1999, Cosenza *et al.* 1993). Damage indices are estimated by comparing the response parameters demanded by the earthquake with the structural capacities. Powell and Allahabadi (1988) proposed a damage index in terms of the ultimate ductility (capacity) μ_u and the maximum ductility μ_{max} demanded by the ground motion

$$D_\mu = \frac{\mu_{max} - 1}{\mu_u - 1} \quad (7)$$

Cosenza *et al.* (1993) and Fajfar (1992) proposed a damage index based on the structure hysteretic energy E_H

$$D_H = \frac{E_H/(f_y u_y)}{\mu_u - 1} \quad (8)$$

Park and co-workers developed a damage index based on maximum ductility and hysteretic energy dissipated by the structure (Park and Ang 1985, Park *et al.* 1987)

$$D_{PA} = \frac{\mu_{max}}{\mu_u} + \beta \frac{E_H/(f_y u_y)}{\mu_u} \quad (9)$$

Here, μ_{max} and E_H are the maximum ductility and hysteretic energy demands (excluding elastic energy). μ_u is the ultimate ductility capacity under monotonic loading and β is a positive constant that weights the effect of cyclic loading on structural damage ($\beta = 0$ implies that the contribution to D_{PA} from cyclic loading is omitted).

The state of the structure's damage is defined as: (a) repairable damage ($D_{PA} < 0.40$), (b) damaged beyond repair ($0.40 \leq D_{PA} < 1.0$) and (c) total or complete collapse ($D_{PA} \geq 1.0$). These criteria are based

on calibration of D_{PA} against experimental results and field observations after earthquakes (Park *et al.* 1987). Eq. (9) expresses damage as a linear combination of the damage caused by excessive deformation and that contributed by repeated cyclic loading effect. Note that the quantities μ_{max} , E_H depend on the loading history while the parameters β , μ_{us} , f_y are independent of the loading history and are determined from experimental tests. The next section develops critical earthquake loads for inelastic structures.

4. Critical earthquake loads considering evolution of seismic waves

The ground acceleration is represented as a combination of N_s seismic waves

$$\ddot{u}_g(t) = \sum_{i=1}^{N_s} e_i(t) \ddot{u}_i(t) = \sum_{i=1}^{N_s} e_i(t) \sum_{j=1}^{N_f} R_{ij} \cos(\omega_{ij}t - \phi_{ij}) \quad (10)$$

Herein, R_{ij} and ϕ_{ij} are unknown amplitudes and phase angles, ω_{ij} is the j th circular frequency of the i th seismic wave and N_f is the number of frequencies considered in each signal. The envelope function of the i th seismic wave is taken to be given as (Conte and Peng 1997)

$$e_i(t) = \alpha_i (t - \xi_i)^{\beta_i} e^{-\lambda_i(t - \xi_i)} \quad (11)$$

where α_i and λ_i are positive constants, β_i is a positive integer, ξ_i is the arrival time of the i th seismic wave. In this study, the ground acceleration is taken to be composed of body waves and surface waves ($N_s = 2$).

In deriving critical earthquake loads, the envelope functions are taken to be known while the amplitudes and phase angles (Eq. (10)) are treated as unknowns. The information on energy E and PGA (M) are also assumed to be known, thus, defining the following constraints (Abbas and Manohar 2002, Moustafa 2009a)

$$\left[\int_0^{\infty} \ddot{u}_g^2(t) dt \right]^{\frac{1}{2}} \leq E \quad (12)$$

$$\max_{0 < t < \infty} |\ddot{u}_g(t)| \leq M$$

Note that the constraint on the earthquake energy is related to the Arias intensity (Arias 1970).

The constraints of Eq. (12) are further expressed in terms of the variables as: R_{ij} , ϕ_{ij} ; $i = 1, 2, \dots, N_s$, $j = 1, 2, \dots, N_f$ as

$$\left[\sum_{i=1}^{N_s} \sum_{j=1}^{N_f} \sum_{m=1}^{N_s} \sum_{n=1}^{N_f} R_{ij} R_{mn} \int_0^{\infty} e_i(t) e_m(t) \cos(\omega_{ij}t - \phi_{ij}) \cos(\omega_{mn}t - \phi_{mn}) dt \right]^{\frac{1}{2}} \leq E$$

$$\max_{0 < t < \infty} \left| \sum_{i=1}^{N_s} e_i(t) \sum_{j=1}^{N_f} R_{ij} \cos(\omega_{ij}t - \phi_{ij}) \right| \leq M \quad (13)$$

To quantify the constraints quantities E and M , it is assumed that a set of acceleration records are available for the given site or from other sites with similar soil conditions. The values of energy and

PGA are obtained for each of these records. The highest of these values across all records are taken to define E and M . It may be noted that the constraints on the Fourier amplitude spectra developed by Abbas and Manohar (2002) require more information on recorded earthquakes at the site and have not been considered here.

The problem of deriving critical earthquake loads for inelastic structures can be posed as determining the optimization variables $\mathbf{y} = \{R_{11}, R_{12}, \dots, R_{N_s N_f}, \phi_{11}, \phi_{12}, \dots, \phi_{N_s N_f}\}^T$ such that D_{PA} (Eq. (9)) is maximized subject to the constraints of Eq. (13). This nonlinear constrained optimization problem is solved using the sequential quadratic programming method (Arora 2004). The following convergence criteria are adopted

$$|f_j - f_{j-1}| \leq \varepsilon_1; |y_{i,j} - y_{i,j-1}| \leq \varepsilon_2 \quad (14)$$

Herein, f_j is the objective function at the j th iteration, $y_{i,j}$ is the i th optimization variable at the j th iteration and $\varepsilon_1, \varepsilon_2$ are small positive quantities to be specified. The structure inelastic deformation is estimated using the Newmark- β method which is built as a subroutine inside the optimization program.

It may be emphasized that the quantities $\mu(t)$ and $E_H(t)$ do not reach their respective maxima at the same time. Hence, the damage index of Eq. (9) is maximized at discrete points of time and the optimal solution $\mathbf{y}^* = \{R_{11}^*, R_{12}^*, \dots, R_{N_s N_f}^*, \phi_{11}^*, \phi_{12}^*, \dots, \phi_{N_s N_f}^*\}^T$ is the one that produces the maximum structural damage at all time points. The next section provides numerical illustrations for the formulation developed above.

5. Numerical results and discussions

We consider a one-storey frame structure. The columns' initial stiffness (storey stiffness) is taken as 4×10^6 N/m and the girder carries a total load of 10^5 kg (initial natural frequency = 1.0 Hz). The columns are taken to behave bilinear inelastic with strain-hardening ratio $\gamma = 0.05$. The yield strength in tension and compression are taken as 6×10^4 N and -6×10^4 N, respectively (yield displacements are 0.02 m and -0.02 m). A viscous damping model with 0.02 damping ratio is adopted. The constraints of Eq. (13) have been quantified using a set of 20 earthquake records (Moustafa 2009a). These records have been recorded at sites with firm soil condition. Specifically, $M = 4.63$ m/s² and $E = 4.16$ m/s^{1.5} (Eq. (12)). The envelope functions adopted (Eq. (11)) are shown in Fig. 1 (Conte and Peng 1997). The numerical values of the parameters of these envelope functions are taken as $\alpha_1 = 2.0, \zeta_1 = 5.0, \beta_1 = 8, \lambda_1 = 0.60$ for body waves and $\alpha_2 = 8.0, \zeta_2 = 2.0, \beta_2 = 6, \lambda_2 = 0.45$ for surface waves. These envelope functions are normalized to unit peak values. Note that the numerical values of the parameters $\zeta_i, i = 1, 2$ are used to control the arrival time of each seismic wave. The numerical values of these parameters are changed later to study the influence of the arrival time of the seismic waves on the derived critical acceleration and the associated inelastic response. Note that the envelope functions can be treated as unknowns and the optimal values of the envelopes parameters can be estimated using optimization techniques. In that case, upper and lower bounds and other positivity constraints on these parameters need to be specified. To quantify these constraints, the numerical values of these parameters have to be calculated for each of the available records to match their nonstationarity trends. The lowest and the highest values of these parameters define the lower and the upper bound constraints. This approach,

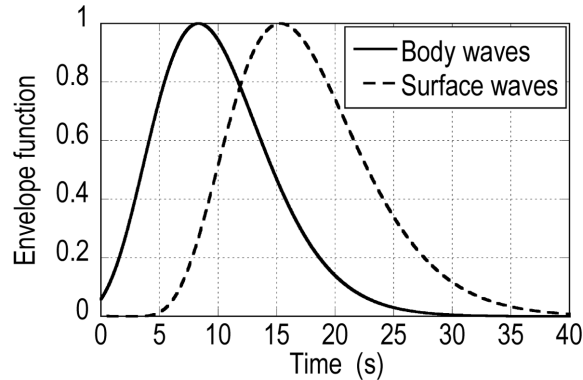


Fig. 1 Envelope functions of body waves and surface waves showing different arrival times

however, may lead to an overly constrained optimization problem or could result in unrealistic nonstationarity trend for the seismic waves, especially with the form of the envelope functions adopted in this paper (large number of envelope parameters). Such approach can be considered for simple envelope functions as has been carried out in some of our previous studies (Takewaki 2004b, Abbas 2006). In this paper, the envelope functions are taken to reflect the average nonstationarity trend of the past recorded accelerograms at the site.

The frequency content of the surface waves is taken as (0-1.0) Hz and that for the body waves is taken as (1.0-10.0) Hz (Okada and Shibata 2008). These frequency ranges are discretized at 0.10 Hz resulting in a total of 204 optimization variables ($N_j = 102$, see Eq. (10)). The influence of the frequency contents of the seismic waves on the estimated critical acceleration and the associated structural response are also studied later. The structure's inelastic response is computed using the Newmark numerical integration scheme ($\alpha = 0.50$; $\delta = 0.25$, $\Delta t = 0.005$ s). The parameters β and μ_u of Eq. (9) are taken as 0.15 and 6.0, respectively. The input energy and the hysteretic, damping, kinetic and elastic strain energies dissipated by the structure are calculated using Eqs. (3)-(6) and the damage indices are computed using Eqs. (7)-(9).

The numerical results are shown in Figs. 2-9 and Tables 1-3. Based on thorough investigations of the numerical results obtained, the following observations are made.

5.1 Non-stationarity trend and effect of arrival time of seismic waves

The body waves have different non-stationarity trend and different arrival time compared with the surface waves (Figs. 2(a),(c)). Body waves build up faster, have relatively narrow strong phase and decay faster. Surface waves build up at about 8.0 s, have longer strong phase and decay slower. These features match the assumed modulating envelope functions and arrival times (see Fig. 1). The two acceleration components result in a total acceleration that has broader strong phase of about 20.0 s. It is also noted that the peak ground acceleration is attained at the overlap time-interval between the peaks of the body waves and the surface waves (see Fig. 2(e)). To examine the influence of the arrival times on the derived critical acceleration and associated structural response, ζ_2 in Eq. (11), that controls the arrival time of the surface waves, has been changed to 2.5, shifting the arrival time and the peak amplitude by about 2.0 s. This was seen to reduce the maximum ductility, the number of yield reversals and the Park and Ang damage index from 1.91, 79 and 4.54 to 1.35, 64 and 2.43, respectively. This implies that, when the arrival times of the seismic waves are

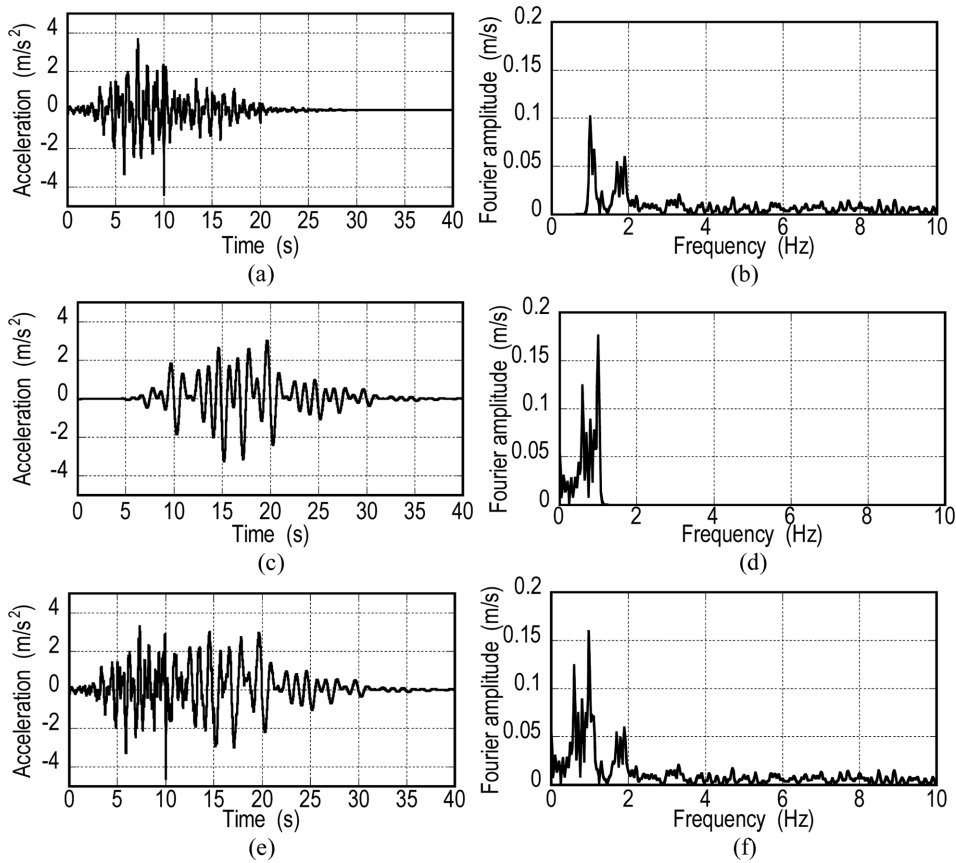


Fig. 2 Critical ground acceleration for bilinear inelastic structure: (a) Body waves in time domain, (b) Body waves in frequency domain, (c) Surface waves in time domain, (d) Surface waves in frequency domain, (e) Total acceleration in time domain, (f) Total acceleration in frequency domain

close, more energies are superposed resulting in larger structural responses (e.g. case of near-field shallow ground motion). When the arrival times are significantly different, the energy of the total acceleration is distributed across a wider time duration (e.g. case of far-field deep earthquakes) leading to smaller responses.

5.2 Frequency content and effect of frequency range of seismic waves

The frequency content of the body waves covers a broad frequency range with significant energy concentrated close to the initial fundamental frequency of the structure. Lower energy is also distributed at higher frequencies (Fig. 2(b)). A similar feature is also observed in the surface waves where large energy is located close to the initial natural frequency of the structure and smaller energy is located at the low frequency range of 0-0.5 Hz (Fig. 2(d)). The resulting ground acceleration is fairly rich in frequency content resembling actual recorded accelerograms (Fig. 2(f)). A peak amplitude is observed at the system initial natural frequency and large amplitudes are located at frequencies lower and higher than the system initial natural frequency (at about half and twice ω). Fig. 3 depicts the short-time Fourier transform of the body waves, the surface waves and

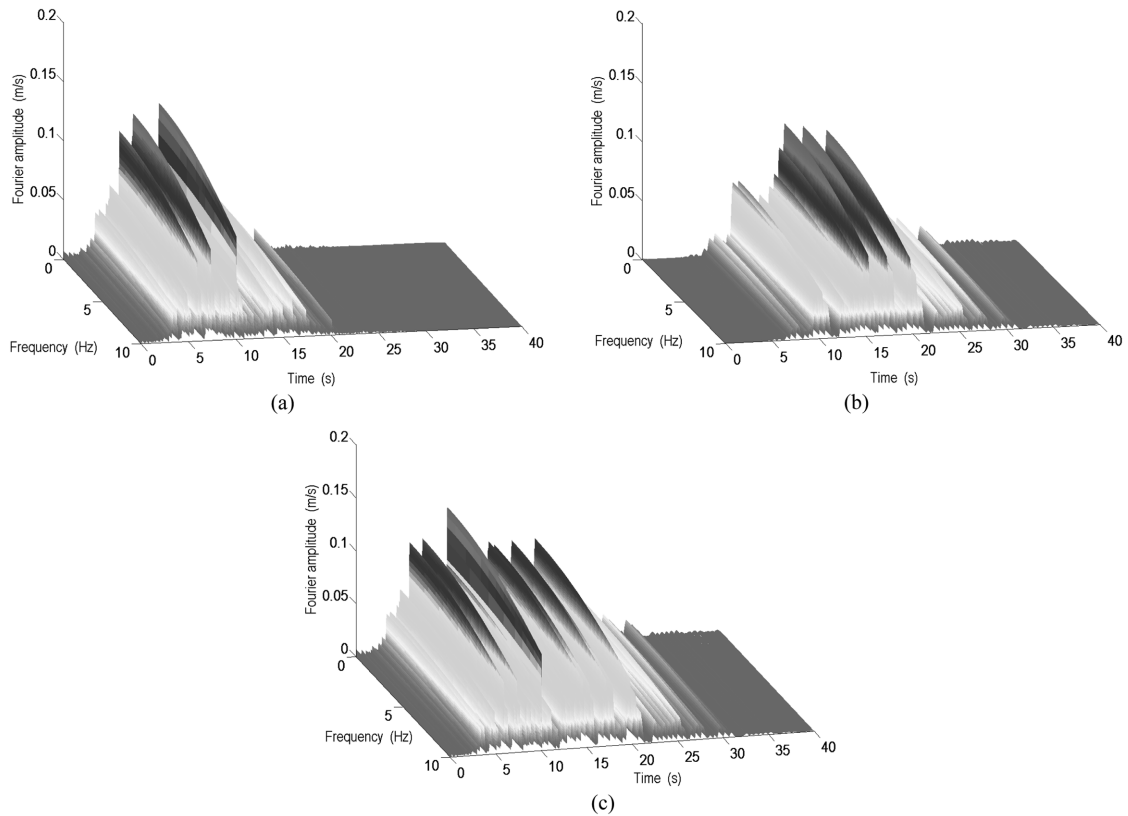


Fig. 3 Short-time Fourier amplitude spectra for the critical ground acceleration: (a) Body waves, (b) Surface waves, (c) Total acceleration

the overall acceleration. The transient trend of the ground motion in time and frequency domains is remarkable. To examine the effect of the frequency contents of the seismic waves on the derived critical acceleration and structural responses, the frequency contents of the surface and body waves have been changed to (0-1.50) Hz and (0.50-10.0) Hz, respectively, keeping all other parameters unchanged. This overlap in the frequency contents of the seismic waves has been seen to lead to ground acceleration that is richer in the frequency content compared with the case studied above. The structural responses have also been seen to increase due to the overlap in the frequency contents of the seismic waves.

5.3 Structural responses

The maximum inelastic response of about 0.39 m is reached at around 16.0 s (Fig. 4(a)). The associated force-displacement hysteretic loops are shown in Fig. 4(b). This is further divided into four time intervals (0-10, 10-20, 20-30 and 30-40 s) and is shown in Figs. 5(a)-(d) (the end of each interval is marked in these plots). It can be seen that the number of yield reversals is higher for the period 10-20 s ($N_y = 28$). The number of yield reversals reduces remarkably at the end of the ground motion ($N_y = 4$ for $t = 30-40$ s). Note also that the hysteretic loops are wider during the interval $t = 10-20$ s and that the maximum displacement is also attained during the same time

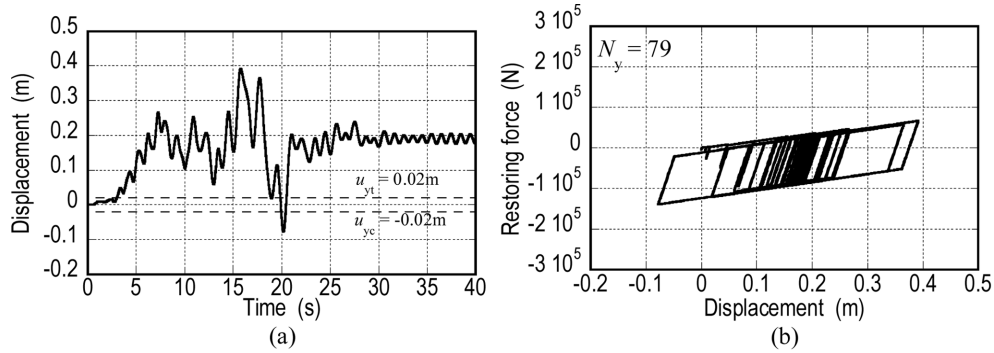


Fig. 4 Response of the inelastic structure under the critical acceleration:
 (a) Inelastic displacement, (b) Force-displacement hysteretic loops

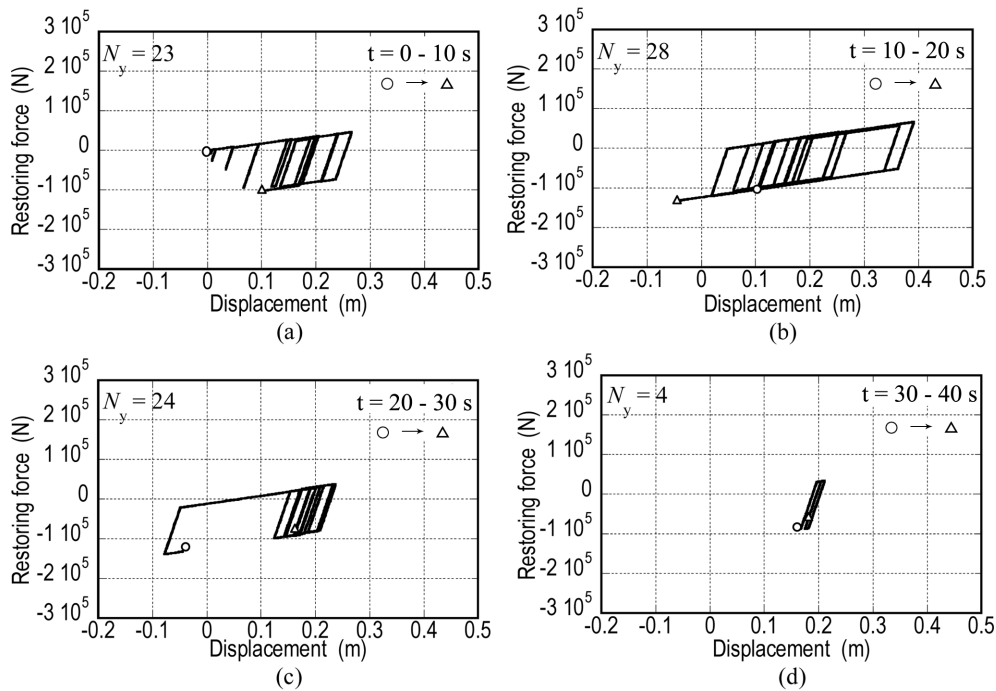


Fig. 5 Force-displacement hysteretic loops for different time intervals: (a) $t = 0-10$ s, (b) $t = 10-20$ s, (c) $t = 20-30$ s, (d) $t = 30-40$ s (\circ and \triangle , represent the extreme points of the hysteretic loops)

period. Most of the input energy to the structure (around 80%) is provided during this period and the maximum value is achieved at about 25 s (Fig. 6). It may also be noted that most of the input energy is dissipated by the hysteretic energy and that the damping energy is significantly smaller (Fig. 6). The kinetic and elastic strain energies are substantially small and diminish at the end of the ground motion. The damage indices reveal that they increase during the strong phase of the ground motion (Fig. 7). Park and Ang damage index reflects that the structure is damaged beyond repair ($D_{PA} = 4.54$). Note that the damage index D_H demanded by the critical input (Eq. (8)) is significantly higher than other two damage indices. The damage index that is based on ductility is the smallest among the three damage indices (0.18).

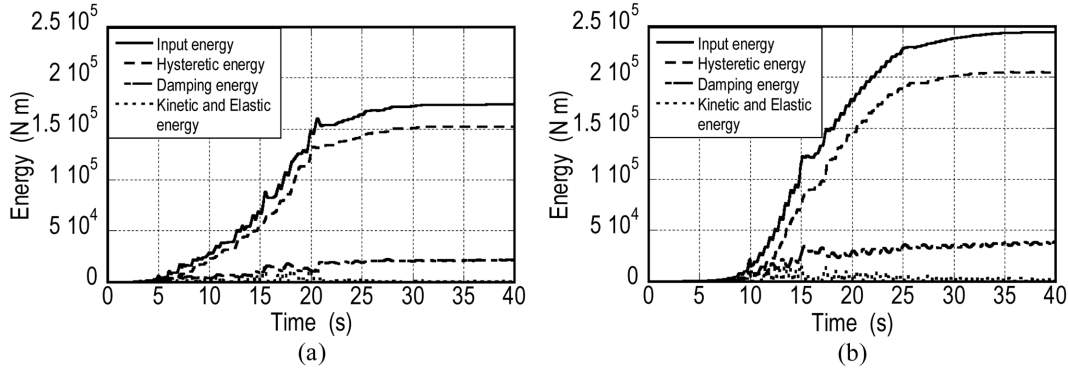


Fig. 6 Input and dissipated energies for the inelastic structures under the critical acceleration: (a) $f_y = 6.0 \times 10^4$ N, (b) $f_y = 12 \times 10^4$ N

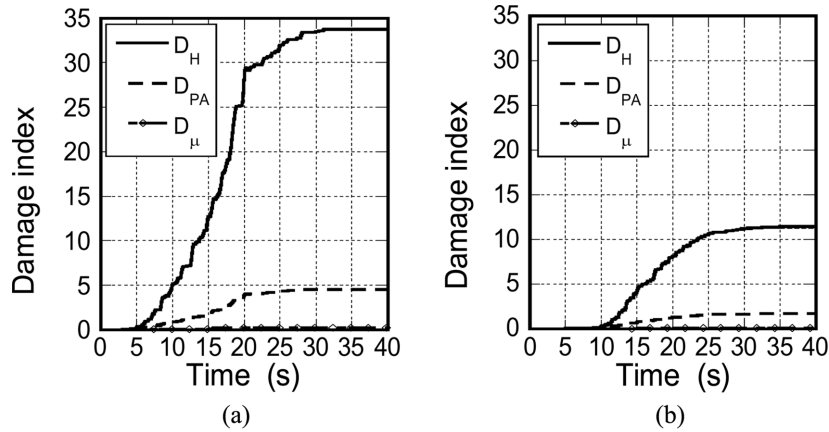


Fig. 7 Damage indices (Eqs. (7)-(9)) for the inelastic structures under the critical acceleration: (a) $f_y = 6.0 \times 10^4$ N, (b) $f_y = 12 \times 10^4$ N (Note that D_μ in Fig. 7(b) coincides with the x-axis)

5.4 Influences of the yield parameters (f_y and γ)

The yield strength is seen to influence the frequency content of the surface waves of the critical acceleration and also the structure input and hysteretic energies. The frequency content of the critical acceleration for the structure with lower yield strength (6×10^4 N) is seen to get shifted towards the lower frequency range (Fig. 8(a)). The structure with higher yield capacity (12×10^4 N) is seen to have higher input energy and hysteretic energy demand (Fig. 6), lower ductility demand and lower damage indices (Fig. 7). For instance, when the yield strength increases from 6×10^4 N to 12×10^4 N, Park and Ang damage index reduces from 4.54 to 1.50. Similarly, the strain-hardening ratio was seen to influence the critical input and the associated inelastic responses. Table 1 summarizes the response quantities for $\gamma = 0.01, 0.05, 0.10$ and 0.50 . It can be seen that, as the strain-hardening ratio decreases the structure yields more frequently and the maximum displacement decreases.

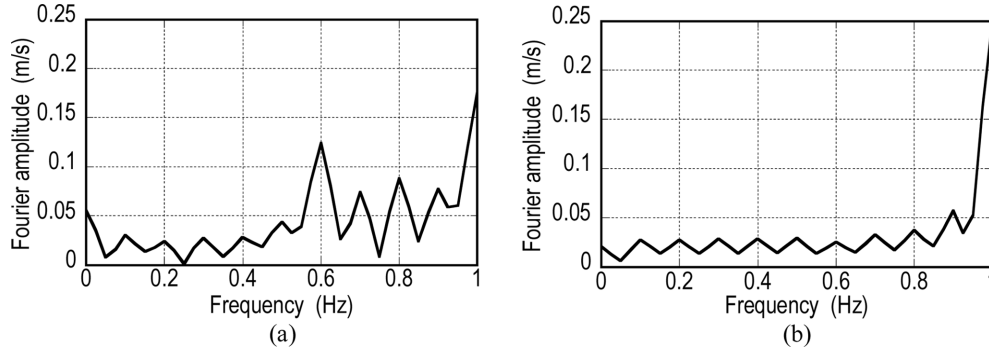


Fig. 8 Influence of the yield strength on the frequency content of the surface waves:
(a) $f_y = 6.0 \times 10^4$ N, (b) $f_y = 12 \times 10^4$ N

Table 1 Influence of the strain-hardening ratio on the response of the inelastic structure

| Strain-hardening ratio | μ_{max} | N_y | u_p (m) | D_{PA} | D_H | D_μ |
|------------------------|-------------|-------|-----------|----------|-------|---------|
| 0.01 | 1.33 | 111 | 0.72 | 3.24 | 24.2 | 0.07 |
| 0.05 | 1.91 | 79 | 0.18 | 4.54 | 33.8 | 0.18 |
| 0.10 | 5.77 | 92 | 0.11 | 5.70 | 37.9 | 0.95 |
| 0.50 | 11.20 | 55 | 0.01 | 3.90 | 16.3 | 2.03 |

μ_{max} = maximum ductility demand, N_y = number of yield reversals, u_p = residual deformation after ground stops shaking, D_{PA} = Park and Ang damage index (Eq. (9)), D_H = Damage index based on hysteretic energy dissipation (Eq. (8)), D_μ = damage index based on ductility (Eq. (7)).

Table 2 Influence of the initial natural frequency on the response of the inelastic structure

| Initial natural frequency | μ_{max} | N_y | u_p (m) | D_{PA} | D_H | D_μ |
|---------------------------|-------------|-------|-----------|----------|-------|---------|
| 0.5 Hz | 2.43 | 66 | 0.22 | 5.23 | 38.6 | 0.29 |
| 1.0 Hz | 1.91 | 79 | 0.18 | 4.54 | 33.8 | 0.18 |
| 2.0 Hz | 1.78 | 56 | 0.08 | 0.36 | 0.50 | 0.16 |

5.5 Effect of initial natural frequency of the structure

To examine the influence of the structure's initial natural frequency on the critical excitation and the associated inelastic response, a parametric study has been carried out. The structure's initial natural frequency is varied, keeping all other parameters unchanged, and the critical input was re-estimated by solving a new optimization problem. Table 2 shows the response parameters of the structure under the critical excitation for three different initial natural frequencies (0.50, 1.0 and 2.0 Hz) with the three structures having the same yield characteristics and damping ratio. It can be seen that the initial natural frequency has significant effect on the critical responses. The structure with lower initial natural frequency produces higher ductility demand and damage indices.

5.6 Comparison with recorded accelerations

To examine the realism of the critical accelerations, the structural responses have been estimated from the critical acceleration and from past recorded ground motions. All acceleration inputs have

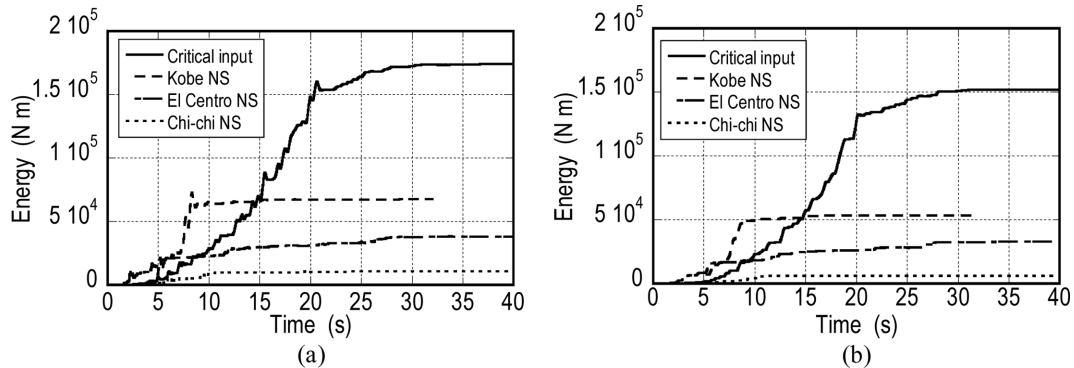


Fig. 9 Input and hysteretic energies from the critical acceleration and past recorded accelerograms (all records are scaled to $PGA = 4.63 \text{ m/s}^2$): (a) Input energy, (b) Hysteretic energy

Table 3 Response quantities for the inelastic structure under the critical acceleration and past recorded ground motions

| Input acceleration | μ_{max} | N_y | u_p (m) | D_{PA} | D_H | D_μ |
|--------------------------------|-------------|-------|-----------|----------|-------|---------|
| Critical acceleration | 1.91 | 79 | 0.18 | 4.54 | 33.8 | 0.18 |
| 1995 Kobe NS (Kobe university) | 1.71 | 26 | 0.29 | 1.76 | 11.8 | 0.14 |
| 1940 El Centro NS (array #9) | 1.98 | 65 | 0.08 | 1.24 | 7.26 | 0.20 |
| 1999 Chi-chi NS (TCU078) | 1.03 | 21 | 0.15 | 0.34 | 1.33 | 0.01 |

been scaled to the same PGA of 4.63 m/s^2 . Fig. 9 and Table 3 show the numerical results. The input energy from the critical input is around 2.5, 4.6 and 16.6 times the associated values from Kobe, El Centro and Chi-chi earthquake records, respectively. On the other hand, the hysteretic energy demand from the critical input is 2.8, 4.7 and 25.6 times those from Kobe, El Centro and Chi-chi records, respectively. It should be remarked that the input energy rate (input energy per unit time) from the critical input is seen to be substantially higher than those from the actual earthquake records (see Takewaki 2006).

6. Conclusions

Strong ground motions are composed of seismic waves that have different characteristics, such as, phase velocity, arrival time, non-stationarity trend, duration, frequency content, energy and amplitude. This paper has investigated the modeling of critical earthquake loads for inelastic structures taking into account the different characteristics of the seismic wave components of the ground acceleration. The critical earthquake loads have been calculated by solving inverse dynamic problems using nonlinear optimization, inelastic time-history analysis and damage indices. The critical acceleration is expressed as a superposition of seismic waves with unknown amplitudes and phase angles. These unknown parameters have been computed such that a measure of the structure's damage is maximized subject to predefined bounds on the ground motion.

Several aspects relevant to the problem have been studied. For instance, the effects of non-stationarity trend, arrival time and frequency content of the seismic waves on the critical ground acceleration and the associated inelastic responses have been examined. Similarly, the influences of

the structural parameters, such as, the initial fundamental natural frequency, the yield strength and the strain-hardening ratio on the structural responses have also been studied. The structural response has been characterized in terms of the maximum ductility, input and hysteretic energies and damage indices. In this context, it may be emphasized that damage indices are accurate response descriptors since they can account for structural damage due to repeated stress reversals and high stress excursions. The critical earthquake load is seen to possess large energy close to the structure's initial natural frequency. Significant energy has also been observed at lower frequencies than the natural frequency of the elastic structure. When the seismic waves have comparable arrival times, the critical acceleration has been seen to produce larger damage in the structure. The structure with lower strain-hardening ratio has been shown to yield more frequently than the same structure with higher strain-hardening ratio. The hysteretic energy has also been seen to increase for lower values of the strain-hardening ratio. In other words, the elastic-plastic structure has been found to be the most vulnerable one. It should be remarked that the input energy rate (input energy per unit time) from the critical input is seen to be substantially higher than those from actual records.

The study has considered that the ground acceleration is composed of two seismic components, namely, body waves and surface waves. Implicit constraints on the frequency contents and the arrival times of the seismic waves have been imposed. Explicit constraints on the energy and peak ground acceleration of the overall ground motion have also been imposed. No constraints were imposed on the energies or the amplitudes of the individual components of the seismic waves. Such constraints can be easily incorporated in the formulation but this information is not easily available. The structures considered have been approximated using single-degree-of freedom systems and the nonlinear behavior has been modeled using bilinear force-displacement relation. The application of the methodology developed in this paper to multi-degree-of-freedom structures and the use of nonlinear degrading models are of interest and will be studied in a future work.

Acknowledgements

This research is partly supported by research funds from the Japanese Society for the Promotion of Science (No. JSPS-P-08073) and the Grant-in-Aid for Scientific Research (No. 21360267). These supports are gratefully acknowledged.

References

- Abbas, A.M. (2006), "Critical seismic load inputs for simple inelastic structures", *J. Sound Vib.*, **296**, 949-967.
- Abbas, A.M. and Manohar, C.S. (2002), "Investigations into critical earthquake load models within deterministic and probabilistic frameworks", *Earthq. Eng. Struct. D.*, **31**(4), 813-832.
- Abbas A.M. and Manohar, C.S. (2007), "Reliability-based vector nonstationary random critical earthquake excitations for parametrically excited systems", *Struct. Safe.*, **29**, 32-48.
- Akiyama, H. (1985), *Earthquake-resistant limit-state design for buildings*, University of Tokyo Press, Tokyo.
- Amiri, G.G. and Dana, F.M. (2005), "Introduction to the most suitable parameter for selection of critical earthquakes", *Comput. Struct.*, **83**(8-9), 613-626.
- Arias, A. (1970), *A measure of earthquake intensity: seismic design of nuclear power plants*, Cambridge, MA, MIT press, 438-468.
- Arora, J.S. (2004), *Introduction to optimum design*, Elsevier Academic Press, San Diego.

- Chopra, A.K. (2007), *Dynamics of structures*, Prentice-Hall, 3rd edition, NJ.
- Conte, J.P. (1992), "Effects of earthquake frequency nonstationarity on inelastic structural response", *Proc. of 10th World Conf. on Earthq. Eng.*, Rotterdam, A.A. Balkema.
- Conte, J.P. and Peng, B.F. (1997), "Fully nonstationary analytical earthquake ground-motion model", *J. Eng. Mech.*, **123**(1), 15-24.
- Cosenza, C., Manfredi, G. and Ramasco, R. (1993), "The use of damage functionals in earthquake engineering: a comparison between different methods", *Earthq. Eng. Struct. D.*, **22**, 855-868.
- Der Kiureghian, A. (1996), "A coherency model for spatially varying ground motions", *Earthq. Eng. Struct. D.*, **25**, 99-111.
- Der Kiureghian, A. and Crempien, J. (1989), "An evolutionary model for earthquake ground motion", *Struct. Safe.*, **6**, 235-246.
- Drenick, R.F. (1970), "Model-free design of aseismic structures", *J. Eng. Mech.*, **96**, 483-493.
- Elnashai, A.S. and Sarno, L.D. (2008), *Fundamentals of earthquake engineering, Chapter 3: Earthquake input motion*, John Wiley & Sons, England.
- Fajfar, P. (1992), "Equivalent ductility factors, taking into account low-cyclic fatigue", *Earthq. Eng. Struct. D.*, **21**, 837-848.
- Ghobara, A., Abou-Elfath, H. and Biddah, A. (1999), "Response-based damage assessment of structures", *Earthq. Eng. Struct. D.*, **28**, 79-104.
- He, W.L. and Agrawal, A.K. (2008), "Analytical model of ground motion pulses for the design and assessment of seismic protective systems", *J. Struct. Eng.*, **134**(7), 1177-1188.
- Hudson, J.A. (1969), "A quantitative evaluation of seismic signals at teleseismic distances-II: body waves and surface waves from an extended source", *Geophys. J. R. Astr. Soc.*, **18**, 353-370.
- Iyengar, R.N. (1970), "Matched inputs", *Report 47, Series J*, Center for Applied Stochastics, Purdue University, West Lafayette, Indiana.
- Lin, Y.K. and Yong, Y. (1987), "Evolutionary Kanai-Tajimi earthquake models", *J. Eng. Mech.*, **113**(8), 1119-1137.
- Meyer, P., Ochsendorf, J., Germaine, J. and Kausel, E. (2007), "The impact of high-frequency/low-energy seismic waves on unreinforced masonry", *Earthq. Spectra*, **23**, 77-94.
- Moustafa, A. (2009a), "Critical earthquake load inputs for multi-degree-of-freedom inelastic structures", *J. Sound Vib.*, **325**, 532-544.
- Moustafa, A. (2009b), "Discussion of a new approach of selecting real input ground motions for seismic design: the most unfavorable real seismic design ground motions", *Earthq. Eng. Struct. D.*, **38**, 1143-1149.
- Moustafa, A. and Takewaki, I. (2009), "Use of probabilistic and deterministic measures to identify unfavorable earthquake records", *J. Zhej. Uni.: Science A*, **10**(5), 619-634.
- Nigam, N.C. and Narayanan, S. (1994), *Applications of random vibrations, Chapter 7: Response of structures to earthquakes*, Narosa Publishing House, New Delhi.
- Okada, K. and Shibata, T. (2008), *Geomechanics*, University of Tokyo Press, Tokyo. (in Japanese)
- Park, Y.J. and Ang, A.H.S. (1985), "Mechanistic seismic damage model for reinforced concrete", *J. Struct. Eng.*, **111**(4), 722-739.
- Park, Y.J., Ang, A.H.S. and Wen, Y.K. (1987), "Damage-limiting aseismic design of buildings", *Earthq. Spectra*, **3**(1), 1-26.
- Powell, G.H. and Allahabadi, R. (1988), "Seismic damage predictions by deterministic methods: concepts and procedures", *Earthq. Eng. Struct. D.*, **16**, 719-734.
- Shinozuka, M. (1970), "Maximum structural response to seismic excitations", *J. Eng. Mech.*, **96**, 729-738.
- Takewaki, I. (2002), "Seismic critical excitation method for robust design: a review", *J. Struct. Eng.*, **128**(5), 665-672.
- Takewaki, I. (2004a), "Bound of earthquake input energy", *J. Struct. Eng.*, **130**, 1289-1297.
- Takewaki, I. (2004b), "Critical envelope functions for non-stationary random earthquake input", *Comput. Struct.*, **82**(20-21), 1671-1683.
- Takewaki, I. (2005), "Resonance and criticality measure of ground motions via probabilistic critical excitation method", *Soil Dyn. Earthq. Eng.*, **21**(8), 645-659.
- Takewaki, I. (2006), "Probabilistic critical excitation method for earthquake energy input rate", *J. Eng. Mech.*,

132, 990-1000.

Takewaki, I. (2007), *Critical excitation methods in earthquake engineering*, Elsevier, Amsterdam, 1-22.

Uang, C.M. and Bertero, V.V. (1990), "Evaluation of seismic energy in structures", *Earthq. Eng. Struct. D.*, **19**, 77-90.

Wang, Z.L., Konietzky, H. and Shen, R.F. (2010), "Analytical and numerical study of P-wave attenuation in rock shelter layer", *Soil Dyn. Earthq. Eng.*, **30**(1-2), 1-7.

Zahrah, T.F. and Hall, W.J. (1984), "Earthquake energy absorption in SDOF structures", *J. Struct. Eng.*, **110**, 1757-1772.

Zhai, C.H. and Xie, L.L. (2007), "A new approach of selecting real input ground motions for seismic design: the most unfavourable real seismic design ground motions", *Earthq. Eng. Struct. D.*, **36**, 1009-1027.

CC